

# Wide-band current preamplifier for conductance measurements with large input capacitance

Andrey V. Kretinin<sup>1,a)</sup> and Yunchul Chung<sup>2,b)</sup>

<sup>1</sup>Condensed Matter Physics Department, Weizmann Institute of Science, Rehovot, Israel

<sup>2</sup>Department of Physics, Pusan National University, Busan 609-735, South Korea

(Received 9 April 2012; accepted 18 July 2012; published online 22 August 2012)

A wide-band current preamplifier based on a composite operational amplifier is proposed. It has been shown that the bandwidth of the preamplifier can be significantly increased by enhancing the effective open-loop gain. The described  $10^7$  V/A current gain preamplifier had the bandwidth of about 100 kHz with the 1 nF input shunt capacitance. The measured preamplifier current noise was  $46 \text{ fA}/\sqrt{\text{Hz}}$  at 1 kHz, close to the design noise minimum. The voltage noise was found to be about  $2.9 \text{ nV}/\sqrt{\text{Hz}}$  at 1 kHz, which is in a good agreement with the value expected for the particular operational amplifier used in the input stage. By analysing the total produced noise we found that the optimal frequency range suitable for the fast lock-in measurements is from 1 kHz to 2 kHz. To obtain the same signal-to-noise ratio, the reported preamplifier requires  $\sim 10\%$  of the integration time needed in measurements made with a conventional preamplifier. © 2012 American Institute of Physics. [<http://dx.doi.org/10.1063/1.4740521>]

## I. INTRODUCTION

Current or transimpedance preamplifier is one of the most commonly used tools for signal acquisition from high-impedance devices under test (DUT) such as photodiodes and bolometers. It is also widely used to measure the low-frequency (10 Hz–100 Hz) conductance of various mesoscopic quantum devices, such as quantum dots,<sup>1</sup> quantum point contacts,<sup>2</sup> and electron interferometers<sup>3</sup> by detecting the device current using the lock-in technique.<sup>4</sup> The overwhelming majority of the mesoscopic quantum devices operate at cryogenic temperatures (below 4.2 K). As a consequence, the cryogenic DUT has to be connected to the room-temperature preamplifier by means of long cryostat signal lines. Apart from that, the signal lines are often heavily filtered to suppress the external RF noise. Hence, the total capacitance across the input becomes relatively large (0.5 nF–5 nF). This large shunting capacitance reduces the measurement bandwidth and increases the overall background noise, which in turn reduces the signal-to-noise ratio (SNR) and requires longer data acquisition time. Therefore, it is important to develop a transimpedance preamplifier, which would provide a wide (dc to  $\sim 100$  kHz) bandwidth with a large ( $\sim 1$  nF) input capacitance.

Recently, Vandersypen *et al.* build the current preamplifier based on a dual low-noise junction field effect transistor (JFET) with the open-loop gain of about  $10^4$  and the current gain of  $10^7$  V/A. They demonstrated the bandwidth exceeding 100 kHz with the 1.5 nF input capacitance.<sup>5</sup> However, it is cumbersome to build a large open-loop operational amplifier (op-amp) using discrete components, moreover the authors did not provide an adequate description of the op-amp circuit itself. Usually, it is not difficult to find an op-amp with high

open-loop gain based on bipolar junction transistors (BJT). Unfortunately, these op-amps produce the input current noise too high (few  $\text{pA}/\sqrt{\text{Hz}}$ ) to be used for a current preamplifier. Meanwhile, op-amps based on a JFET input stage have rather low current noise (at least three orders of magnitude smaller than that of BJT), but small open-loop gain. To overcome these complication, we used a so-called composite op-amp,<sup>6</sup> which is a cascaded low-noise JFET op-amp input stage and a wide-band current-feedback op-amp. This realization makes it much easier to build a wide-band current amplifier with a low input noise.

In this report we present a simple transimpedance preamplifier based on a composite op-amp design, which was built using the bipolar field-effect transistor (BiFET) AD743 op-amp as the low-noise input stage, and the high-speed current-feedback AD811 op-amp as a gain booster. The increased open-loop gain allowed us to extend the bandwidth up to 100 kHz at 1 nF input capacitance with the current gain of  $10^7$  V/A. The total current and voltage noise of the preamplifier measured at 1 kHz were  $46 \text{ fA}/\sqrt{\text{Hz}}$  and  $2.9 \text{ nV}/\sqrt{\text{Hz}}$  correspondingly, which are comparable to the values reported for the current preamplifier built from discrete JFETs.<sup>5</sup>

## II. THE BANDWIDTH OF A CURRENT PREAMPLIFIER

First, we would like to discuss the factors determining the bandwidth of an op-amp based transimpedance preamplifier. Figure 1 shows the equivalent circuit of the preamplifier formed by an op-amp with the gain bandwidth  $f_{\text{gbw}}$ , and the feedback network  $R_f C_f$ . The DUT is represented by the resistor  $R_s$  shunted with the input capacitance  $C_L$ . The meaning of the current and voltage noise sources will be discussed in Sec. IV.

The transimpedance preamplifier is prone to be unstable, especially with large input capacitance, hence it requires some feedback compensation with  $C_f$ . The preamplifier

<sup>a)</sup>Present address: School of Physics and Astronomy, University of Manchester, Manchester M13 9PL, United Kingdom.

<sup>b)</sup>Author to whom correspondence should be addressed. Electronic mail: [ycchung@pusan.ac.kr](mailto:ycchung@pusan.ac.kr).

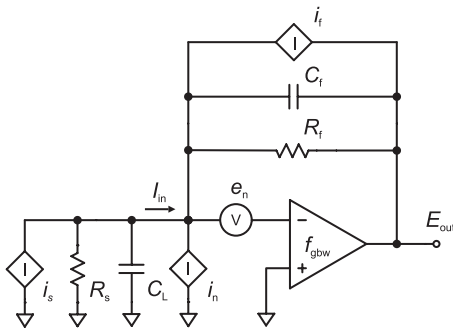


FIG. 1. The full equivalent circuit of the transimpedance inverting preamplifier formed by the operational amplifier with gain bandwidth  $f_{\text{gbw}}$  and feedback network  $R_f C_f$ . The device under test is modeled with the resistor  $R_s$  connected by the signal line with capacitance  $C_L$ .

transfer function is  $V_{\text{out}} = -I_{\text{in}} \cdot R_f [1 + (\omega R_f C_f)^2]^{-1/2}$ , where  $\omega = 2\pi f$ , and it defines the high-frequency cutoff as

$$f_c = \frac{1}{2\pi R_f C_f}. \quad (1)$$

The choice of the  $C_f$  value is dictated by the stability considerations, and determined by the value of  $C_L$  coupled to the input. Indeed, for the circuit in Fig. 1 to be stable the feedback zero frequency  $f_z = (2\pi(R_s \parallel R_f)(C_L + C_f))^{-1}$  should be inside the open-loop gain curve defined as  $A = f_{\text{gbw}}/f$ .<sup>7</sup> The largest stable bandwidth in this case is set by the condition  $A \cdot \beta = 1$  at  $f = f_c$ , where  $\beta$  is the feedback factor.<sup>8</sup> This condition is used to find an optimal value of the feedback capacitance, under condition  $R_s C_L \ll R_f C_f$ ,

$$C_f = \sqrt{\frac{C_L}{2\sqrt{2}\pi f_{\text{gbw}} R_f}}. \quad (2)$$

As seen from Eqs. (1) and (2) the input capacitance  $C_L$  reduces the amplifier bandwidth, hence a high open-loop gain op-amp is needed to compensate for this reduction. Alternatively, one can reduce the value of  $R_f$ , but in this case SNR will be seriously compromised since it is proportional to  $\sqrt{R_f}$ . Indeed, if the input signal is  $I_{\text{in}}$ , and the dominant background noise is limited by the thermal fluctuations of  $R_f$  as  $I_{\text{noise}} = \sqrt{4k_B T/R_f}$ , the resulting ratio is  $\text{SNR} = I_{\text{in}}/I_{\text{noise}} \propto \sqrt{R_f}$ .

Another limitation for the transimpedance preamplifier bandwidth comes from the fact that the op-amp gain is finite, and the shunting capacitance  $C_L$  affects the transfer function. The naive explanation would be that at higher frequencies the input current  $I_{\text{in}}$  is shunted by  $C_L$ , and part of it is diverted to the ground, bypassing the current preamplifier with the effective input impedance  $R_{\text{in}} = R_f/(1 + A)$ .<sup>9</sup> In this case the  $-3$  dB cut-off frequency is

$$f_{-3\text{dB}} = \sqrt{\frac{(\sqrt{2} - 1)f_{\text{gbw}}}{2\pi R_f C_L}} = f_c \sqrt{(\sqrt{2} - 1) \frac{C_f}{C_L} \frac{f_{\text{gbw}}}{f_c}}. \quad (3)$$

Note, that for any reasonable situation  $C_L \gg C_f$  and  $f_{\text{gbw}} \gg f_c$ , hence  $f_{-3\text{dB}} < f_c$  and the real-situation bandwidth is determined by Eq. (3) rather than by Eq. (1), unless the feedback network is overcompensated ( $C_f$  is larger than the optimal value given by Eq. (2)). It is clear from Eqs. (1) and (3) that

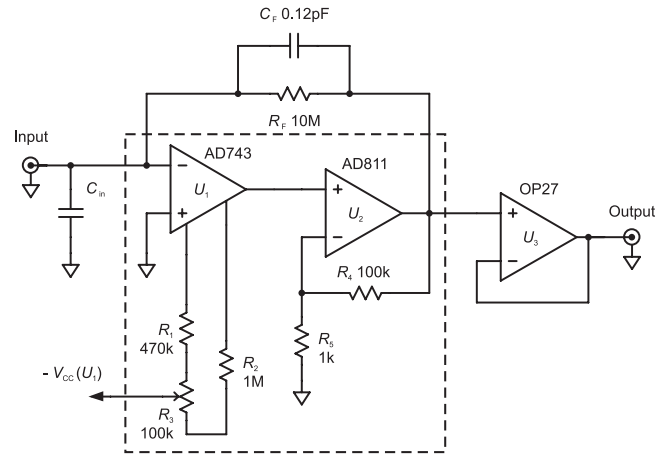


FIG. 2. The circuit diagram of the composite current preamplifier with the current gain  $10^7$  V/A. The composite op-amp circuit is marked by the dashed box. In order to minimise the parasitic stray capacitance the preamplifier was assembled on a surface mount printed circuit board and enclosed in an aluminium box. All the components used were of the surface-mount type; the 1206 surface mount device (SMD) metal-film resistors (Philips Electronics), 0805 SMD ceramic and 1210 SMD tantalum capacitors (AVX), and the op-amps in small-outline integrated circuit (SOIC)-type package (analog devices).

the only way to compensate the bandwidth reduced by  $C_L$  is to increase the open-loop gain of the op-amp.

### III. COMPOSITE OP-AMP CURRENT AMPLIFIER

Most of the commercial JFET input op-amps, which are suitable for the current preamplifier application, have relatively small gain bandwidth. For example, an ultralow-noise high-speed AD743 op-amp<sup>10</sup> has excellent input noise characteristics, but rather low gain bandwidth  $f_{\text{gbw}} = 4.5$  MHz. Therefore, it is unsuitable for wide-band applications, since the preamplifier bandwidth with a 1 nF shunt capacitor and  $R_f = 10^7 \Omega$  would be about 10 KHz. To overcome this problem we adopted the so-called composite op-amp design.<sup>6</sup> The circuit diagram of our composite amplifier is shown in Fig. 2. As an input stage we used the ultralow-noise AD743 op-amp,  $U_1$ . The input stage is followed by the gain booster build on a non-inverting voltage gain  $10^2$  amplifier,  $U_2$ . Both stages share common feedback network  $R_f C_f$ , and form the composite op-amp (enclosed in the dashed box in Fig. 2) with the gain bandwidth enhanced by a factor  $10^2$  resulting in  $f_{\text{gbw}} = 450$  MHz. The preamplifier is completed with the voltage buffer,  $U_3$ .

Several op-amps were tested as the gain booster, and the current-feedback video op-amps usually gave better high-frequency characteristics. However, setting the booster gain higher than  $10^2$  usually caused the circuit instability. To reduce the stray capacitance of the feedback resistor  $R_f$  was made of five 2 M $\Omega$  metal-film resistors connected in series. The value of  $C_f$  was found experimentally by stabilising the preamplifier with the 1 nF capacitor connected to the input. The nominal value of  $C_f = 0.12$  pF is close to that found from Eq. (2) ( $\sim 0.15$  pF), and it was achieved by the series connection of four 0.47 pF surface mount ceramic capacitors. The open-input capacitance  $C_{\text{in}}$  was estimated to be about 47 pF.

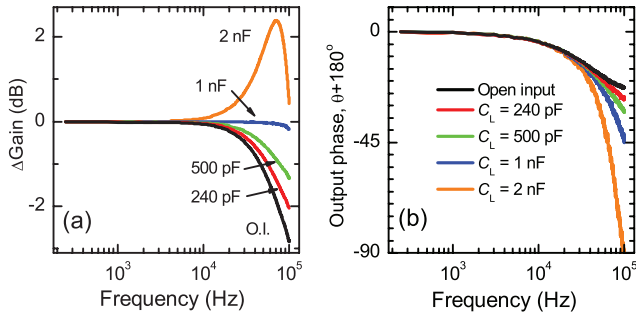


FIG. 3. The frequency response of the composite current preamplifier shown in Fig. 2. (a) The measured gain flatness at different values of the input capacitance  $C_L$  presented by the normalized gain  $\Delta\text{Gain} = 20 \log(-V_{\text{out}}/I_{\text{in}}R_f)$ . (b) The signal phase frequency response at different values of the input capacitance  $C_L$ . The value of  $C_L$  increases for curves from top to bottom.

Apart from a pair of ceramic and electrolyte decoupling capacitors (47 nF and 10  $\mu\text{F}$ , correspondingly) connected to the power supply pins of every op-amp, the power lines were heavily filtered with  $LC$  low-pass filters, or with the feedthrough  $\pi$ -sections filters mounted onto the preamplifier chassis. To decouple from the low-frequency mains power interference, the preamplifier was fed by a pair of 12 V lead-acid batteries.

The frequency response of our preamplifier measured at different values of the input capacitance  $C_L$  is presented in Fig. 3. Figure 3(a) shows the gain flatness given by the normalized gain  $\Delta\text{Gain} = 20 \log(-V_{\text{out}}/I_{\text{in}}R_f)$ . As seen from the plot, the open-input gain (marked as “O.I.”) has its cut-off frequency slightly above 100 kHz. The preamplifier gain has excellent flatness up to  $f \approx 10$  kHz, and exhibits some peaking only when  $C_L$  exceeds 1 nF.

The gain overshoot masks the  $-3$  dB cut-off point, therefore it is not straight forward to determine the bandwidth of the amplifier. To do this we used the signal phase frequency response, and found the bandwidth as the frequency at which the signal phase shift is  $45^\circ$ .<sup>11</sup> From the frequency response shown in Fig. 3 it is seen that the preamplifier bandwidth is around 100 kHz for 1 nF input capacitance, which is comparable to that of the current amplifier built using discrete JFETs.<sup>5</sup> Further improvement of the bandwidth can be achieved by using JFET op-amps with larger  $f_{\text{gbw}}$ , such as AD745 and AD8610.

In our search for alternative op-amps we considered only those, which have the possibility to balance the input offset voltage. The offset voltage builds up between the inputs of the op-amp due to the mismatch of the input transistors parameters, and usually amounts to about 1 mV. The presence of the offset voltage results in an unintentional bias of the DUT. In the case of mesoscopic quantum transport systems at milli-Kelvin temperature, such as a quantum dot in the Kondo regime,<sup>13</sup> even a small (few microvolts) dc bias would alter the strongly non-linear conductance, thus the input offset voltage should be properly compensated. The input offset voltage of the preamplifier can be adjusted by balancing the first stage op-amp with a conventional trimming circuit  $R_1 \div R_3$  ( $R_3$  is the Vishay Spectrol 10-turn wirewound-type potentiometer). This circuit allows to null the offset voltage to within  $\pm 1 \mu\text{V}$

( $\sim k_B T/e$  at  $T = 10$  mK). The stability of the offset voltage is mainly determined by the thermal drift of the op-amp, and the quality of the preamplifier power supply. In our specific case the thermal drift was eliminated by a 30-min warm up, and the long-time stability was limited by the discharge rate of the lead-acid batteries. Normally, a 2.1 A·h battery provides at least 48 h of the stable ( $\pm 1 \mu\text{V}$ ) offset voltage operation.

#### IV. NOISE CHARACTERISTICS

In the equivalent circuit of the preamplifier shown in Fig. 1 all components are assumed to be noiseless. The current and voltage fluctuations in the circuit are introduced by adding corresponding voltage and current noise sources. Here we consider the composite op-amp as a single entity, which is characterised by its equivalent input voltage ( $e_n$ ) and current ( $i_n$ ) noise.<sup>12</sup> Another source of noise in the circuit is the thermal fluctuations of the feedback resistor  $R_f$  given by the current noise density  $i_f = \sqrt{4k_B T/R_f}$ . The presence of the DUT also contributes to the total noise through the thermal fluctuations of  $R_s$  with current density  $i_s = \sqrt{4k_B T/R_s}$ . Assuming that all sources of noise are uncorrelated and the op-amp gain  $A$  is large, the square of total output voltage noise density  $V_n^2$  can be written as

$$\begin{aligned} V_n^2 &= \frac{R_f^2}{1 + (\omega R_f C_f)^2} \cdot I_n^2 \\ &= \frac{R_f^2}{1 + (\omega R_f C_f)^2} \left[ i_s^2 + i_f^2 + i_n^2 + e_n^2 \left( \frac{1}{R_s} + \frac{1}{R_f} \right)^2 \right. \\ &\quad \left. + e_n^2 (\omega(C_L + C_f))^2 \right]. \end{aligned} \quad (4)$$

Here  $I_n$  is the total input current noise density, and the prefactor  $R_f^2[1 + (\omega R_f C_f)^2]^{-2}$  accounts for the finite bandwidth of the preamplifier.

To characterise the preamplifier noise and quantify the contribution of each of the noise sources we measured the thermal noise spectral density of several different metal-film resistors  $R_s$  at  $T = 4.2$  K. These resistors were placed on the experimental probe inside the liquid  $^4\text{He}$  dewar. Each of the resistor was connected by a coaxial cable producing the total shunt capacitance  $C_L = 438$  pF. The values of  $R_s$  were chosen to be close to the values typical for mesoscopic quantum devices ( $R_s \geq G_0^{-1} \approx 12.9$  k $\Omega$ , where  $G_0 = 2e^2/h$  is the conductance quantum).<sup>1-3</sup> The noise spectral density was measured with SR770 FFT Spectrum Analyzer (Stanford Research Systems). In order to increase SNR of the noise measurements, we used an additional low-noise voltage preamplifier (LI-75A, NF Corporation) in series with the tested current preamplifier.

The total current noise spectral density  $I_n$  measured for different  $R_s$  is shown in Fig. 4(a). On the same figure we plotted the current noise spectrum for the open-input preamplifier (marked as “O.I.”). The open-input noise represents the minimal possible noise of the current preamplifier, and it is estimated to be about 46 fA/ $\sqrt{\text{Hz}}$ . This noise consists of the thermal noise of the feedback resistor  $i_f$ , and the current

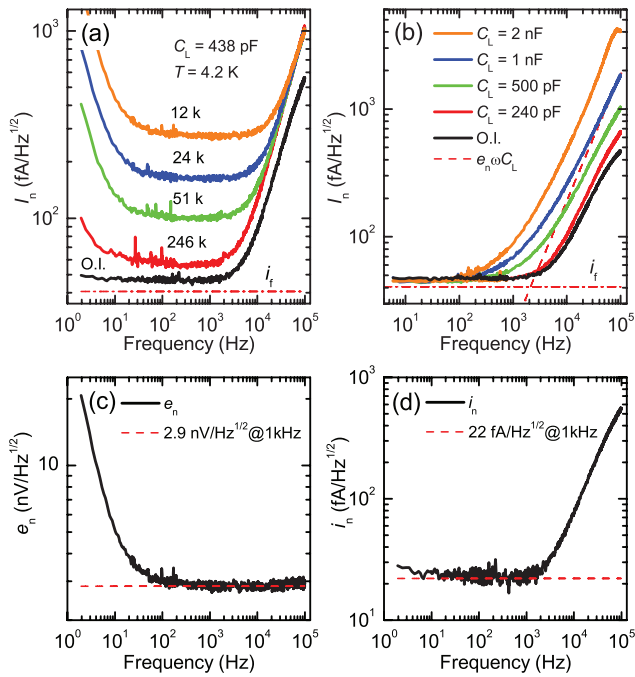


FIG. 4. The noise characterisation of the composite current preamplifier shown in Fig. 2. (a) The preamplifier total noise density spectrum measured for the open input (“O.I.”) and different values of  $R_s$  (12 k $\Omega$ , 24 k $\Omega$ , 51 k $\Omega$ , 246 k $\Omega$ ).  $R_s$  was immersed in liquid  $^4\text{He}$  ( $T = 4.2$  K) and connected by the coaxial cable with  $C_L = 438$  pF. The red dash dotted line represents the thermal noise of the feedback resistor  $R_f$  ( $i_f = 41$  fA/ $\sqrt{\text{Hz}}$ ). (b) The total current noise of the open-input preamplifier measured for different input capacitances  $C_L$ . The dashed line shows the current noise expected from coupling of the voltage noise  $e_n = 2.9$  nV/ $\sqrt{\text{Hz}}$  through the capacitor  $C_L = 1$  nF. The dash dotted line represents the thermal noise of the feedback resistor the same as in (a). (c) and (d) The extracted op-amp voltage ( $e_n$ ) and current ( $i_n$ ) noise density spectra, correspondingly.

noise of the composite op-amp  $i_n$  (contribution from the voltage noise  $e_n$  is negligibly small). As seen from Fig. 1(a), the thermal noise of  $R_f$  ( $\sim 41$  fA/ $\sqrt{\text{Hz}}$ ), shown by the dash dotted line, is a dominant contributor and defines the absolute noise floor. The high-frequency increase observed at  $f > 2$  kHz is typical for the current noise of a FET, and originates from the thermal noise of the transistor channel coupled to the input through the gate-to-drain capacitance.<sup>12</sup> As expected from Eq. (4) the total noise increases if DUT and the cable are connected to the preamplifier. The increase occurs due to the contribution from the thermal noise  $i_s$ , and the coupling of the voltage noise of the op-amp  $e_n$  through the resistance  $R_s$  and the capacitance  $C_L$  (last two terms in Eq. (4)). The thermal noise of DUT is independent on frequency and adds equally to the whole spectrum. The voltage noise, on the contrary, has a  $1/f$  component<sup>12</sup> which is responsible for the noise increase at  $f < 100$  Hz. The relatively frequency-independent minimum of the total noise at a given  $R_s$  occurs in the frequency range from 100 Hz to 2 kHz. This noise floor is mainly determined by the contribution from  $i_s$  and  $e_n/R_s$ . At higher frequencies ( $f > 2$  kHz) the voltage noise of the op-amp also couples through the input capacitance as  $e_n\omega(C_L + C_f)$ , and adds to the increasing high-frequency noise, initially brought by the op-amp current noise  $i_n$ . Despite the fact that the capacitor is noiseless, the input voltage noise coupled to the

input capacitor introduces a significant share of the total noise, which is often overlooked. To demonstrate how  $e_n$  is coupled through the input capacitance, we measured the total noise of the preamplifier with only  $C_L$  connected to the input. Figure 4(b) clearly shows that the high-frequency current noise increases with the increasing capacitance  $C_L$  due to larger contribution from the op-amp voltage noise. Assuming that the voltage source  $e_n$  does not contribute to the open-input noise, and the thermal noise of  $R_f$  and  $R_s$  is known, one can extract the spectral density of the op-amp noise. Figures 4(c) and 4(d) show the spectrum of the voltage ( $e_n$ ) and current ( $i_n$ ) noise of the op-amp, correspondingly. As noticed before,  $e_n$  has a  $1/f$  component for  $f < 100$  Hz and becomes frequency independent at higher frequencies. The voltage noise density at 1 kHz is found to be about 2.9 nV/ $\sqrt{\text{Hz}}$ , which is the value expected for the voltage noise of AD743, and determined by the thermal noise of the input FET channel.<sup>10</sup> The current noise  $i_n$  is frequency independent up to 2 kHz with the minimum noise density of about 22 fA/ $\sqrt{\text{Hz}}$  at 1 kHz, which is about 3 times higher than that expected for the current noise of AD743. Most likely, the discrepancy originates from the unaccounted noise of the gain booster stage of the composite op-amp.

Figure 4(a) gives an idea on the optimal frequency range suitable for the lock-in measurements<sup>4</sup> with this current preamplifier. It is clear that the lowest total noise occurs in the range from 1 kHz to 2 kHz. The advantage of higher lock-in reference frequency is that it allows to avoid the low-frequency  $1/f$ -noise, and to reduce the lock-in integration time (provided SNR is high enough), which makes the measurements faster. The excellent frequency response and noise characteristics made it possible to use the described current preamplifier in real mesoscopic transport experiments on one-dimensional conductors<sup>14</sup> and quantum dots<sup>15</sup> performed at milli-Kelvin temperatures. The lock-in measurements using the composite preamplifier at  $\sim 1$  kHz with 30 ms integration time gave SNR comparable to that obtained with the conventional current preamplifier (ITHACO 1211) at frequencies below 100 Hz and 300 ms integration time.

We would like to mention alternative techniques used to decrease the noise and increase the bandwidth of two-terminal conductance measurements. Since the total preamplifier noise is determined mostly by the thermal fluctuations, it is logical to reduce the operational temperature of the feedback network and the input circuitry. Dereniak *et al.*<sup>16</sup> realized the background-limited photoconductive detector by cooling the feedback resistor to the liquid  $^4\text{He}$  temperature. This approach is effective only when the DUT impedance is high, and the contribution from the voltage noise of the input FET is negligible. To overcome the difficulty of large voltage noise the input FET stage has to be cold as well. Several successful attempts were made to build current preamplifiers with cold input FET stage.<sup>17</sup>

Recently, there has been suggested a so-called RF reflectometry technique, which is an indirect high-speed low-noise tool to measure the two-terminal conductance.<sup>18</sup> In this technique the DUT is a part of the resonant LCR circuit, and the DUT conductance is extracted from the resonator quality factor. The RF reflectometry started to gain its popularity in the high-speed mesoscopic transport experiments.<sup>19</sup> Though

all the methods mentioned above can be used for high-speed precision measurements they require modification of the cryostat wiring, use of cryogenic circuitry, and complex RF equipment.

## V. CONCLUSION

A simple low-noise wide bandwidth current preamplifier based on the composite operational amplifier is proposed. The composite operational amplifier has been employed to increase the open-loop gain. The composite part was implemented by a low-noise BiFET input stage followed by a non-inverting high-speed voltage gain booster with the common feedback network. The designed preamplifier had current gain  $10^7$  V/A, and showed the bandwidth up to 100 kHz with 1 nF capacitor across the input. Apart from the wide bandwidth, the described preamplifier demonstrated excellent noise characteristics. The preamplifier current noise of  $46 \text{ fA}/\sqrt{\text{Hz}}$  at 1 kHz is close to the absolute minimum defined by the thermal noise of the feedback resistor. The voltage noise was measured to be  $2.9 \text{ nV}/\sqrt{\text{Hz}}$  and shown to give a significant contribution to the total current noise when the DUT resistance and input capacitance are finite. The proposed current preamplifier was proven to be an excellent tool for mesoscopic quantum transport experiments.

## ACKNOWLEDGMENTS

Authors thank Moty Heiblum and Hadas Shtrikman for making this work possible at Braun Center for Submicron Research. We also thank Vladimir Umansky and Diana Mahalu for helpful discussions and experimental support. This work was partially supported by the National Research Foundation of Korea (NRF) grant funded by the Korea government (Grant No. 2011-0003109) and the Korea Science and Engineering Foundation (KOSEF) grant funded by the Korea government (Grant No. 2010-0000268).

<sup>1</sup>U. Meirav, M. A. Kastner, and S. J. Wind, *Phys. Rev. Lett.* **65**, 771 (1990).

<sup>2</sup>B. J. van Wees, H. van Houten, C. W. J. Beenakker, J. G. Williamson, L. P. Kouwenhoven, D. van der Marel, and C. T. Foxon, *Phys. Rev. Lett.* **60**, 848 (1988); D. A. Wharam, T. J. Thornton, R. Newbury, M. Pepper, H. Ahmed,

J. E. F. Frost, D. G. Hasko, D. C. Peacock, D. A. Ritchie, and G. A. C. Jones, *J. Phys. C* **21**, L209 (1988).

<sup>3</sup>A. Yacoby, R. Schuster, and M. Heiblum, *Phys. Rev. B* **53**, 9583 (1996).

<sup>4</sup>J. H. Scofield, *Am. J. Phys.* **62**, 129 (1994).

<sup>5</sup>L. M. K. Vandersypen, J. M. Elzerman, R. N. Schouten, L. H. W. van Beveren, R. Hanson, and L. P. Kouwenhoven, *Appl. Phys. Lett.* **85**, 4394 (2004).

<sup>6</sup>W. Mikhael and S. Michael, *IEEE Trans. Circuits Syst.* **34**, 449 (1987); T. Kalthoff, T. Wang, and R. M. Stitt, *Classical Op-Amp or Current Feedback Op-Amp? This Composite Op Amp Gives you the Best of Both Worlds*, Application Bulletin AB-007A No. SBOA002 (Burr-Brown Corporation, 1991).

<sup>7</sup>T. Wang and B. Erhman, *Compensate Transimpedance Amplifiers Intuitively*, Application Report No. SBOA055A (Texas Instruments, Inc., 2005).

<sup>8</sup>The feedback factor  $\beta$  is the part of the output voltage applied to the input through the feedback network, and at  $f = f_c$  is  $\beta = V_{in}/V_{out} = \frac{\sqrt{2}}{2}$ .

<sup>9</sup>The transfer function in case of large  $C_L$  is  $V_{out} = -I_{in} \cdot R_f[\omega R_{in} C_L + \sqrt{1 + (\omega R_f C_f)^2}]^{-1}$ .

<sup>10</sup>AD743 *Ultralow Noise BiFET Op Amp* (Data Sheet), Analog Devices, 2003.

<sup>11</sup>P. Horowitz and W. Hill, *The Art of Electronics*, 2nd ed. (Cambridge University Press, 1989).

<sup>12</sup>C. D. Motchenbacher and J. A. Connelly, *Low Noise Electronic System Design* (Wiley, 1993).

<sup>13</sup>D. Goldhaber-Gordon, H. Shtrikman, D. Mahalu, D. Abusch-Magder, U. Meirav, and M. Kastner, *Nature (London)* **391**, 156 (1998); W. van der Wiel, S. De Franceschi, T. Fujisawa, J. Elzerman, S. Tarucha, and L. Kouwenhoven, *Science* **289**, 2105 (2000).

<sup>14</sup>A. V. Kretinin, R. Popovitz-Biro, D. Mahalu, and H. Shtrikman, *Nano Lett.* **10**, 3439 (2010).

<sup>15</sup>A. V. Kretinin, H. Shtrikman, D. Goldhaber-Gordon, M. Hanl, A. Weichselbaum, J. von Delft, T. Costi, and D. Mahalu, *Phys. Rev. B* **84**, 245316 (2011).

<sup>16</sup>E. L. Dereniak, R. R. Joyce, and R. W. Capps, *Rev. Sci. Instrum.* **48**, 392 (1977).

<sup>17</sup>D. Yvon, V. Sushkov, R. Bernard, J. Bret, B. Cahan, O. Cloue, O. Maillard, B. Mazeau, J. Passerieux, B. Paul, and C. Veyssiere, *Nucl. Instrum. Methods Phys. Res. A* **481**, 306 (2002); C. H. Yang, T. H. Chang, M. J. Yang, and W. J. Moore, *Rev. Sci. Instrum.* **73**, 2713 (2002); D. Antonio, H. Pastoriza, P. Julián, and P. Mandolesi, *ibid.* **79**, 084703 (2008).

<sup>18</sup>R. J. Schoelkopf, P. Wahlgren, A. A. Kozhevnikov, P. Delsing, and D. E. Prober, *Science* **280**, 1238 (1998).

<sup>19</sup>D. R. Schmidt, C. S. Yung, and A. N. Cleland, *Appl. Phys. Lett.* **83**, 1002 (2003); H. Qin and D. A. Williams, *ibid.* **88**, 203506 (2006); M. C. Cassidy, A. S. Dzurak, R. G. Clark, K. D. Petersson, I. Farrer, D. A. Ritchie, and C. G. Smith, *ibid.* **91**, 222104 (2007); L. J. Taskinen, R. P. Starrett, T. P. Martin, A. P. Micolich, A. R. Hamilton, M. Y. Simmons, D. A. Ritchie, and M. Pepper, *Rev. Sci. Instrum.* **79**, 123901 (2008); T. Müller, B. Küng, S. Hellmüller, P. Studerus, K. Ensslin, T. Ihn, M. Reinwald, and W. Wegscheider, *Appl. Phys. Lett.* **97**, 202104 (2010).